Anal. Chem. **2006,** *78,* 8028−8035

Low-Power Concentration and Separation Using Temperature Gradient Focusing via Joule Heating

Sun Min Kim,*,† Greg J. Sommer,† Mark A. Burns,‡,§ and Ernest F. Hasselbrink†

Department of Mechanical Engineering, Department of Chemical Engineering, and Department of Biomedical Engineering, University of Michigan, Ann Arbor, Michigan 48109-2125

We present an experimental study of temperature gradient focusing (TGF) exploiting an inherent Joule heating phenomenon. A simple variable-width PDMS device delivers rapid and repeatable focusing of model analytes using significantly lower power than conventional TGF techniques. High electric potential applied to the device induces a temperature gradient within the microchannel due to the channel's variable width, and the temperature-dependent mobility of the analytes causes focusing at a specific location. The PDMS device also shows simultaneous separation and concentration capability of a mixture of two sample analytes in less than 10 min. An experiment combining Joule heating with external heating/cooling further supports the hypothesis that temperature is indeed the dominant factor in achieving focusing with this technique.

Species preconcentration and separation are significant challenges in the design of microfluidic chemical analysis systems. In a typical electrophoretic separation, the sample concentration is often too dilute for adequate detection. This lack of sensitivity results in either an inaccurate reading or a considerable waste of a limited sample volume.

Several preconcentration techniques have been developed and studied. Many methods trap the analyte against a porous membrane that prohibits the passing of large molecules such as DNA.[1−4] Other methods rely on the establishment of a field gradient to suppress the mobility of the analyte at a single location. For example, isoelectric focusing is a commonly used technique that focuses an analyte at its specific isoelectric point along a pH gradient,[5,6] and isotachophoresis uses variable ion mobility zones for sample focusing.[7] Similar methods rely on electric field gradients to suppress the net analyte velocity at a point in a channel.[8,9] While powerful, many of these techniques are difficult to apply to a broad range of analytes due to the specificity of the method to a certain type of molecule.

Microfluidic temperature gradient focusing (TGF) is a new field gradient focusing method introduced by Ross and Locascio in 2002.[10] TGF is a technique that focuses and separates charged analytes by balancing electrophoretic velocity against the bulk velocity of the buffer. The electrophoretic mobility of a charged species is highly temperature-dependent. TGF exploits this property to suppress the net analyte velocity (electrophoretic + bulk) at a certain location along a temperature gradient, resulting in a concentration of species at that unique point. Ross and Locascio demonstrated successful focusing using both external heating and cooling as well as Joule heating along a variable cross-sectional area microchannel. Because electrophoretic mobility is a unique property of a given analyte, TGF allows for species separation by concentrating different analytes at unique locations along the temperature gradient. The technique has been successfully used to achieve DNA hybridization[11] and chiral separations.[12]

TGF is an excellent technique for concurrent signal enhancement and separation of a mixture of analytes; however, it currently has certain shortcomings which limit its specificity and applicability. From the standpoint of device miniaturization, the main issue is energy consumption: previous TGF approaches use external heating and cooling equipment to establish a temperature gradient along a channel. Establishing a temperature gradient across the entire chip requires a significant amount of energy; for example, two 1 × 1 cm thermoelectric devices, with coefficient of performance of ∼1.5, require at least 2 kJ of energy to maintain a 50 °C temperature difference across a chip for 5 min.[13] Assuming 50% of the analysis cycle is devoted to TGF, this corresponds to only five runs if powered by a typical cell phone battery, and this does not account for other power requirements (such as the HV power supplies). This limits the technique's applicability to portable applications. In this paper, we demonstrate the use of Joule heating within the buffer itself, which although it still uses high voltage, uses much less power and energy per analysis due to the lack of external heating/cooling elements.

* To whom correspondence should be addressed. Phone: (734) 936-0343. Fax: (734) 936-0343. E-mail: sunmk@umich.edu.

† Department of Mechanical Engineering.

‡ Department of Chemical Engineering.

§ Department of Biomedical Engineering.

(1) Khandurina, J.; Jacobson, S. C.; Waters, L. C.; Foote, R. S.; Ramsey, J. M. *Anal. Chem.* **1999**, *71*, 1815−1819.
(2) Foote, R. S.; Khandurina, J.; Jacobson, S. C.; Ramsey, J. M. *Anal. Chem.* **2005**, *77*, 57−63.
(3) Wang, Y. C.; Stevens, A. L.; Han, J. Y. *Anal. Chem.* **2005**, *77*, 4293−4299.
(4) Han, J. Y.; Craighead, H. G. *Anal. Chem.* **2002**, *74*, 394−401.
(5) Bjellqvist, B.; Ek, K.; Righetti, P. G.; Gianazza, E.; Gorg, A.; Westermeier, R.; Postel, W. *J. Biochem. Biophys. Methods* **1982**, *6*, 317−339.
(6) Righetti, P. G.; Bossi, A. *Anal. Chim. Acta* **1998**, *372*, 1−19.
(7) Gebauer, P.; Bocek, P. *Electrophoresis* **2002**, *23*, 3858−3864.
(8) Petsev, D. N.; Lopez, G. P.; Ivory, C. F.; Sibbett, S. S. *Lab Chip* **2005**, *5*, 587−597.
(9) Huang, Z.; Ivory, C. F. *Anal. Chem.* **1999**, *71*, 1628−1632.
(10) Ross, D.; Locascio, L. E. *Anal. Chem.* **2002**, *74*, 2556−2564.
(11) Balss, K. M.; Ross, D.; Begley, H. C.; Olsen, K. G.; Tarlov, M. J. *J. Am. Chem. Soc.* **2004**, *126*, 13474−13479.
(12) Balss, K. M.; Vreeland, W. N.; Phinney, K. W.; Ross, D. *Anal. Chem.* **2004**, *76*, 7243−7249.
(13) In http://www.melcor.com/OptoTEC_%20Series/1.5-31-F2A.PDF.

10.1021/ac061194p CCC: $33.50
Published on Web 10/25/2006

A secondary concern with TGF is that specific buffers are required; the more commonly used buffers will normally yield negligible or highly unstable focusing. In this paper, although we do not look at a wide variety of buffers, we do illustrate a simple step-by-step approach to designing a TGF system for a set of analytes that can predict whether an analyte can be focused a priori. We hope that this assay development methodology accelerates the rate of TGF's adoption as an analytical technique.

Underlying both of these aims is a need for rule-of-thumb prediction of thermal characteristics of TGF-based microdevices, especially the prediction of temperature distributions and criteria for stable focusing. In this paper, we also show that it is possible to combat poor resolution via a secondary electrophoretic separation. In a follow-up paper, we will delve further into computational prediction of temperature distribution and mass transport (e.g., focusing rates, and the width of focused bands).

THEORY

Temperature gradient focusing works analogously to isoelectric focusing. The bulk fluid velocity, u_{bulk}, arising from electroosmotic flow (EOF), pressure-driven flow, or both opposes the electrophoretic drift velocity, u_{ep}, of an analyte. Since u_{ep} is a function of temperature, T, if we make T a function of x (a coordinate along the length of the channel), then u_{ep} is a function of x. The net velocity, $u_{net} = u_{bulk} + u_{ep}$, can be manipulated to achieve focusing at a specific location along a channel if $u_{net} = 0$ and $(\partial u_{net})/(\partial x) < 0$. Conversely, if $(\partial u_{net})/(\partial x) > 0$ at the spot where $u_{net} = 0$, then depletion occurs.

Assuming that convection controls the location of focusing and diffusion effects control the width of the focused band, the quasi 1-D transport equation for the concentration of a species, c, at any location i along the channel can be written (ignoring diffusion):

$$A_i \frac{\partial c_i}{\partial t} = -\frac{\partial}{\partial x}\left[A_i(u_{bulk,i}c_i + u_{ep,i}c_i)\right] \tag{1}$$

where A is the cross-sectional area of the channel. Simplifying this equation using the continuity condition, $\partial(u_{bulk}A)/\partial x = 0$, (assuming constant mass density of the solution) yields:

$$A_i\left[\frac{\partial c_i}{\partial t} + (u_{bulk,i} + u_{ep,i})\frac{\partial c_i}{\partial x}\right] = -c_i\frac{\partial}{\partial x}(A_i u_{ep,i}) \tag{2}$$

At steady state, $\partial c_i/\partial t = 0$, and the resulting differential equation can be solved to yield

$$\frac{c_{x=x1}}{c_{x=x0}} = \frac{(u_{bulk,x0} + u_{ep,x0})A_{x0}}{(u_{bulk,x1} + u_{ep,x1})A_{x1}} \tag{3}$$

Thus, when the net velocity at x_1 is zero, the concentration theoretically approaches $\pm\infty$, but diffusion and dispersion (ignored in the above analysis) will, of course, prevent the singularity from occurring in reality.

The electrophoretic and electroosmotic mobilities, μ_{ep} and μ_{eof}, are temperature-dependent due primarily to the varying viscosity of the buffer solution, and ζ potential of the channel surface,[14] with temperature. This phenomenon allows for a variable u_{net}, and proper device design will yield focusing along the microchannel.

In this work, the temperature gradient will be created by exploiting the Joule heating effect within the bulk fluid due to the applied electric field. If the microchannel is much smaller than the medium in which it is formed (e.g., the glass substrate), the 1-D steady heat-transfer equation, considering only Joule heating within the channel and radial heat conduction away from the channel, can be written in an approximate form, assuming the channel is much wider than its depth:[15]

$$\frac{I^2}{\sigma_i(T_i)d_i w_i} = Kk\frac{T_i - T_\infty}{d_i}w_i \tag{4}$$

where I is the current through the channel, $\sigma(T)$ is the electrical conductivity, d is a length scale on the order of the depth of the microchannel, w is the channel width, k is the thermal conductivity of the glass surrounding the microchannel, and K (which is $O(1)$) accounts for the geometry of the microchannel. If we assume that σ is roughly proportional to temperature difference above ambient, then the temperature varies approximately inversely with the square of the channel width. Thus, regions of narrower cross-sectional area along the channel will reach higher temperatures, and a temperature gradient is induced. This simple rule-of-thumb estimate forms the design basis of our system.

Previous work by Pawliszyn et al. used a similar technique to create a pH profile through Joule heating-induced temperature gradients in a tapered channel for isoelectric focusing; however, the technique explored in this work relies on a direct dependence of a species' electrophoretic mobility with temperature.[16−18]

EXPERIMENTAL SECTION

Materials. The 900 mM Tris−borate buffer (900 mM Tris, 900 mM boric acid, pH 8.0) and phosphate buffer (dibasic sodium phosphate, 20 mM, pH 7.2) solutions were used for the buffer systems. Fluorescein isothiocyanate conjugate bovine serum albumin (FITC−BSA; Sigma-Aldrich, St. Louis, MO) and fluorescein−Na (Sigma-Aldrich) were used for focusing experiments, and each sample was diluted with the buffer solution at several concentrations (100 nM, 25 μM, 0.1 mM). Rhodamine B dye (Molecular Probes) diluted with the 900 mM Tris−borate buffer was used to measure the temperature distribution in the microchannel. Protein sample was kept in a freezer to prevent deterioration, and all liquid samples were filtered with a 0.1-μm syringe filter (Whatman, Maidstone, UK) to remove particulates.

Microchip Fabrication. The microchannel system in Figure 1 was fabricated by casting poly(dimethylsiloxane) (PDMS) over an SU-8 photoresist (SU 8-2010, MicroChem Inc., Newton, MA) mold on a silicon substrate fabricated by photolithography as previously described.[19−22] Briefly, a mixture of the PDMS prepolymer and the curing agent (Sylgard 184, Dow Corning,

(14) Evenhuis, C. J.; Guijt, R. M.; Macka, M.; Marriott, P. J.; Haddad, P. R. *Electrophoresis* **2006**, *27*, 672−676.
(15) Incropera, F. P.; Dewitt, D. P. *Fundamentals of Heat and Mass Transfer*, 5 ed.; John Wiley & Sons, Inc: New York, 2001.
(16) Pawliszyn, J.; Wu, J. Q. *J. Microcolumn Sep.* **1993**, *5*, 397−401.
(17) Fang, X. H.; Adams, M.; Pawliszyn, J. *Analyst* **1999**, *124*, 335−341.
(18) Huang, T. M.; Pawliszyn, J. *Electrophoresis* **2002**, *23*, 3504−3510.

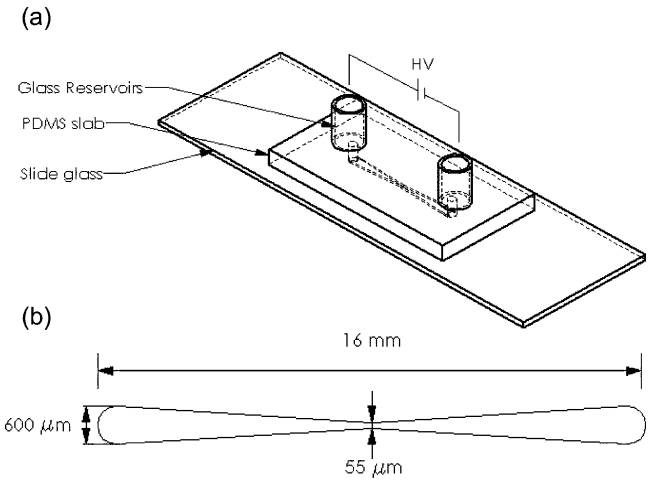

Figure 1. Schematic drawing of experimental microdevice and geometrical profile of corresponding microchannel. (a) The microdevice is composed of a PDMS slab with a patterned microchannel, a slide glass substrate, and two sample reservoirs. (b) The microchannel is 55 μm at its narrowest spot (middle) and 600 μm at its widest spots (ends). The total length of channel is 16 mm and the depth is 18 μm.

Midland, MI) was prepared and degassed. A 5:1 mass ratio of prepolymer and curing agent was used to increase the rigidity of the cured PDMS slab, as described previously.[23,24] The uncured mixture was poured over the mold in a Pyrex Petri dish ~4 mm thick and cured for 1 h at 150 °C. The cured PDMS was detached from the mold and 2-mm-diameter holes for reservoirs were punched vertically through the slab. The PDMS slab with a designed microchannel pattern and a slide glass substrate were treated with an air plasma of 100 W RF power in ~200 mTorr vacuum using a PlasmaPrepII system (SPI supplies, West Chester, PA) for 3 min, then contacted together, and heated at 150 °C for 15 min to create an irreversible bond.[19,20] Cylindrical glass reservoirs (1 cm long, 5-mm inner diameter) were bonded concentrically over the holes on the PDMS slab using UV-curable optical adhesive (Norland, New Brunswick, NJ) with a UV lamp for 10 min.

Temperature Measurement. The temperature gradient inside a microchannel produced by Joule heating was measured with a fluorescence thermometry method previously described.[25–27] Briefly, electric field was applied to a microchannel filled with a 900 mM Tris−borate buffer containing diluted rhodamine B dye, which has a strongly temperature-dependent quantum efficiency, through platinum electrodes (A-M Systems, Carlsborg, WA) placed in the reservoirs using a high-voltage power supply (PS350, Stanford Research Systems, Sunnyvale, CA). The fluorescence intensity of the rhodamine B was monitored using an inverted fluorescence microscopic system (IX-71, Olympus) equipped with a spectral filter set for rhodamine B (excitation, 500−550 nm; emission, >565 nm) and a 100-W mercury lamp. A CCD camera (Hamamatsu) was mounted on the microscope for image acquisition, and IPLab 3.6 software (Scanalytics, Fairfax, VA) was used for camera control and image processing. To prevent photobleaching, a neutral density filter (ND 1.0, Omega Optical, Brattleboro, VT) was installed to reduce excitation light intensity. The ratio of the fluorescence intensity after applying an electric field to the intensity of the initial state (room temperature) was used to calculate the temperature at each point of the microchannel using a calibration curve generated from the intensity measurement with a thermostated silica capillary.

Temperature-Dependent Mobility Measurements. The electrophoretic and net mobilities, $\mu_{ep}(T)$ and $\mu_{net}(T)$, were measured using a photobleached dye imaging method similar to techniques previously described.[28–30] The ends of 10-cm-long × 50-mm-inner diameter capillaries were connected to plastic tubing, and a small viewing region was created in the center of the capillary using a razor blade. The entire system was rinsed with DI water for 5 min, flushed with air, filled with the analyte/buffer solution, and secured along the bottom of a thermal water bath with a viewing window sitting above an inverted fluorescent microscope. The reservoirs were also held in the thermal bath to ensure that the entire capillary system was maintained at the same temperature.

To measure the fluid velocity through the capillary, a small region of the capillary was exposed to a focused laser beam (496 nm, 200 mW, Melles Griot Series 43 Ion Laser, Carlsbad, CA) for 3 s using an electronic shutter controller (ThorLabs SC10, Newton, NJ). The photobleaching creates a concise dark region within the fluorescent sample. Upon removal of the laser beam, electric potential was immediately applied through platinum electrodes in the reservoirs and the migration of the photobleached region was captured at a known frame rate (typically 100 ms/frame) through a CCD camera using image processing software (NI Vision Assistant 7.1.1, National Instruments). An in-house-written Matlab (Mathworks, Natick, MA) code was used to determine the velocity of the photobleached region by finding the axial location of the darkest region in the channel in each image from a known frame rate, from which the mobility can be determined using $\mu = u/E$.

To measure the electrophoretic mobility, $\mu_{ep}(T)$, 50-μm-inner diameter Zero Flow fused-silica capillaries (MicroSolv, Long Branch, NJ) were used. These capillaries are coated internally to suppress the EOF in the channel. Regular, uncoated 50-μm-inner diameter fused-silica capillaries (Polymicro Technologies, Phoenix, AZ) were used to measure $\mu_{net}(T)$. The electroosmotic mobility was then calculated using the relation $\mu_{net}(T) = \mu_{eof}(T) + \mu_{ep}(T)$. To verify the EOF suppression in the coated capillaries, the photobleached velocity method was employed using rhodamine

(19) Duffy, D. C.; McDonald, J. C.; Schueller, O. J. A.; Whitesides, G. M. *Anal. Chem.* **1998**, *70*, 4974−4984.
(20) McDonald, J. C.; Duffy, D. C.; Anderson, J. R.; Chiu, D. T.; Wu, H. K.; Schueller, O. J. A.; Whitesides, G. M. *Electrophoresis* **2000**, *21*, 27−40.
(21) McDonald, J. C.; Metallo, S. J.; Whitesides, G. M. *Anal. Chem.* **2001**, *73*, 5645−5650.
(22) McDonald, J. C.; Chabinyc, M. L.; Metallo, S. J.; Anderson, J. R.; Stroock, A. D.; Whitesides, G. M. *Anal. Chem.* **2002**, *74*, 1537−1545.
(23) Armani, D.; Liu, C.; Aluru, N. In *Mems '99: 12th IEEE International Conference on Micro Electro Mechanical Systems, Technical Digest*; 1999; pp 222−227.
(24) Chang, W. J.; Akin, D.; Sedlak, M.; Ladisch, M. R.; Bashir, R. *Biomed. Microdevices* **2003**, *5*, 281−290.
(25) Lou, J. F.; Finegan, T. M.; Mohsen, P.; Hatton, T. A.; Laibinis, P. E. *Rev. Anal. Chem.* **1999**, *18*, 235−284.
(26) Sakakibara, J.; Adrian, R. J. *Exp. Fluids* **1999**, *26*, 7−15.
(27) Ross, D.; Gaitan, M.; Locascio, L. E. *Anal. Chem.* **2001**, *73*, 4117−4123.
(28) Schrum, K. F.; Lancaster, I. J. M.; Johnston, S. E.; Gilman, S. D. *Anal. Chem.* **2000**, *72*, 4317−4321.
(29) Mosier; Molho; Santiago, E. R. *Exp. Fluids* **2002**, *33*, 545−554.
(30) Sinton, D. E. *Microfluidics Nanofluidics* **2004**, *1*, 2−21.

110 diluted in either buffer solution. Since this is a zwitterionic dye, it can only be transported by bulk flow (EOF). The measured EOF was <4% of that in the uncoated capillaries; therefore, it was neglected in our analysis.

Focusing Measurement. The focusing of FITC−BSA and fluorescein−Na was performed in the microchannel shown in Figure 1. The device was treated with air plasma of 100-W rf power in ~200 mTorr vacuum for 90 s to enhance the hydrophilicity of the channel surface. The microchannel and each reservoir were then filled with DI water and flushed out to clean the channel. The buffer solution used for diluting the sample was introduced into the channel to capture a background image for image processing and flushed out after 5 min. The microchannel and reservoirs were then filled with sample solution, and platinum electrodes were placed in each reservoir to apply the electric field. Fluorescence imaging of the sample was acquired by the same fluorescence microscopic system described in the temperature measurement section, equipped with a different filter set (488 nm) for FITC and fluorescein.

For the combined Joule heating and external heating focusing experiments, two small thermoelectric heat sinks (Melcor OT 1.5−31-F2A, Trenton, NJ) were placed on the bottom of the glass substrate using thermal grease (Cool-Grease, Melcor) to promote conduction, attached to a $^1/_4$-in.-thick copper block, and operated by a dc power supply (Tektronix PS280, Beaverton, OR). During either operation (cooling or heating), the same power was applied to both heat sinks to ensure that the heat flux to the glass substrate was as uniform as possible. For reliable quantification of the sample, all experiments were performed with a fresh new device to prevent nonspecific binding of labeled protein on the channel surface,[31−34] and corrections for background were implemented.

RESULTS AND DISCUSSION

The experiments conducted in the present work were performed with two primary goals. First, bulk fluid and molecular electrophoretic mobilities are measured at various temperatures in different buffers to illuminate the advantage certain buffers have in achieving TGF. Second, a microdevice was fabricated to show that concentration and separation via TGF can be achieved very simply by utilizing the electric potential through a microchannel to provide a temperature gradient via Joule heating. This device is then combined with an external heating/cooling system to show both the effect of temperature on the focusing capability and that TGF can be performed with more commonly used buffers.

Mobility and Temperature Measurements. The electrophoretic and net mobilities, $\mu_{ep}(T)$ and $\mu_{net}(T)$, of 0.1 mM fluorescein−Na were measured in both 900 mM Tris−borate buffer and 20 mM phosphate buffer using the photobleached dye imaging method described earlier (see Supporting Information, Figure SP1). To ensure that no pressure-driven flow was present in the system, tests were completed in which the velocity was measured with no applied external field. Measurements at temperatures ranging from 25 to 79 °C were achievable with the experimental apparatus. The electroosmotic mobility, $\mu_{eof}(T)$, was calculated using the relation $\mu_{eof}(T) = \mu_{net}(T) - \mu_{ep}(T)$.

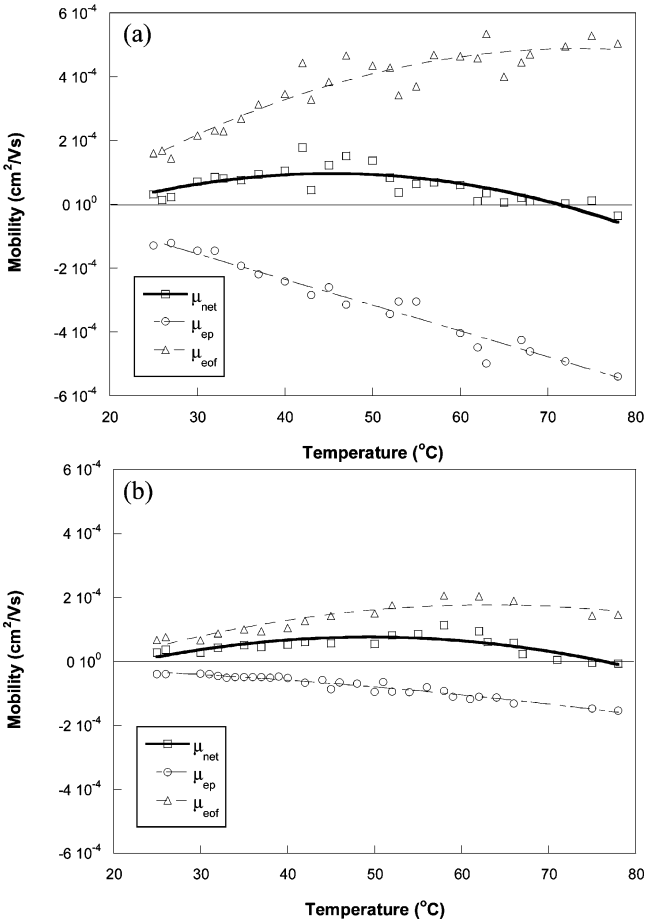

Figure 2. Temperature-dependent mobility profile of 0.1 mM fluorescein−Na in (a) 900 mM Tris−borate buffer and (b) 20 mM phosphate buffer. The square markers represent the net mobility variations of the fluorescein−Na, and the circle markers represent the electrophoretic mobility variations. The electroosmotic mobility (triangle markers) is calculated by subtracting the electrophoretic mobility from the net mobility. Each line is a second-order polynomial fitted curve.

Figure 2a shows that, as expected, the magnitude of $\mu_{ep}(T)$ increases with temperature in the 900 mM Tris−borate buffer. The curve exhibits the inverse proportionality of μ_{ep} with viscosity of the buffer throughout the entire temperature range. The $\mu_{net}(T)$ curve shows that electroosmosis dominates the migration of the sample at low temperatures. At ~50 °C, however, the curve begins to decrease toward zero, and at temperatures of >~70 °C, the net mobility is idle and even shows that electrophoresis may dominate at high temperatures. Note that while $\mu_{ep}(T)$ continues increasing at high temperatures, $\mu_{eof}(T)$ appears to plateau.

Similar trends are seen in Figure 2b for the 20 mM phosphate buffer. However, the magnitudes of the mobilities and $\partial\mu_{net}/\partial T$ are less than half those seen in Figure 2a. The shallower $\partial\mu_{net}/\partial T$ gradient suggests that focusing will be more difficult with this buffer. A steeper $\partial\mu_{net}/\partial T$, such as that for the 900 mM Tris−borate buffer, corresponds to a steeper $\partial u_{net}/\partial x$ along the channel and both an increased probability of focusing and an increased concentration magnitude.

(31) Hu, S. W.; Ren, X. Q.; Bachman, M.; Sims, C. E.; Li, G. P.; Allbritton, N. *Anal. Chem.* **2002**, *74*, 4117−4123.
(32) Makamba, H.; Kim, J. H.; Lim, K.; Park, N.; Hahn, J. H. *Electrophoresis* **2003**, *24*, 3607−3619.
(33) Hu, S. W.; Ren, X. Q.; Bachman, M.; Sims, C. E.; Li, G. P.; Allbritton, N. *Electrophoresis* **2003**, *24*, 3679−3688.
(34) Hu, S. W.; Ren, X. Q.; Bachman, M.; Sims, C. E.; Li, G. P.; Allbritton, N. L. *Anal. Chem.* **2004**, *76*, 1865−1870.

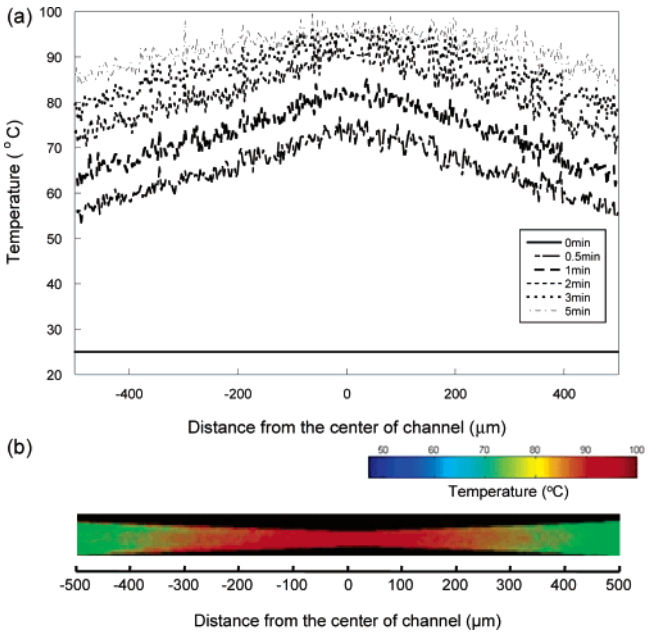

Figure 3. Temperature profile of 900 mM Tris−borate buffer in the analog shape microchannel due to an applied electric potential of 1200 V and the temperature distribution at 5 min. (a) Temperature profile along centerline of microchannel. (b) Temperature distribution at 5 min after applying 1200 V (inverse false color image of rhodamine B solution in channel).

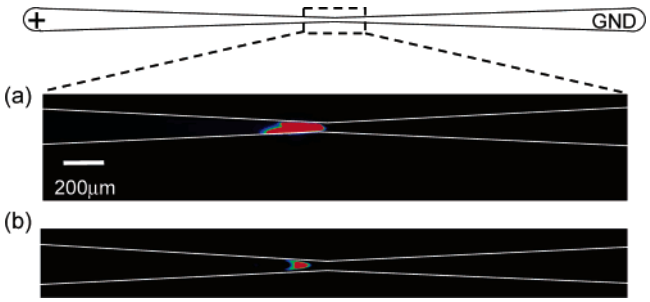

Figure 4. Images after 5 min of sample analyte focusing with an applied electric potential of 1200 V in individual runs. (a) Focusing of 25 μM fluorescein−Na in 900 mM Tris−borate buffer. (b) Focusing of 100nM FITC−BSA in same buffer solution. Each image is a magnified view of the middle region of the microchannel. Approximate E-field in center region of channel, 2.5 × 10^3 V/cm.

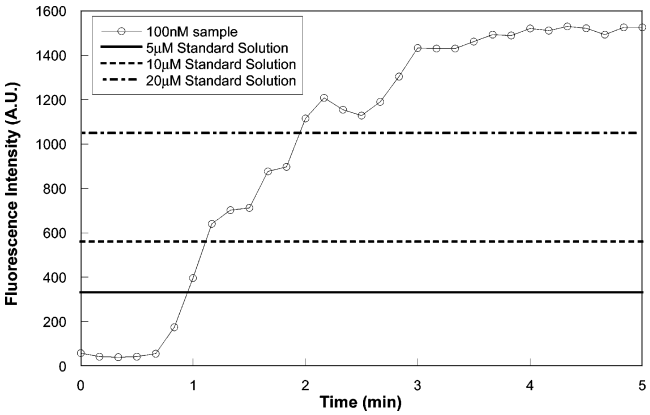

Figure 5. Concentration of 100nM FITC−BSA due to applied 1200 V in analog microchannel. Concentration of 100 nM sample is compared with standard concentration samples (5, 10, and 20 μM). At least 200-fold concentration was achieved in 2 min. Fluorescence intensity is measured at the location of maximum intensity along centerline of microchannel.

The temperature increase within the microchannel is generated by the inherent Joule heating effect from an applied electric potential. The cross-sectional area variations of our microchannel create a temperature gradient because the current density of a narrow part of the channel is higher than it is in the wider part, leading to a temperature change inversely proportional to the square of the channel diameter or width.

The temperature within the microchannel was measured using the temperature-dependent fluorescence intensity of 0.1 mM rhodamine B in 900 mM Tris−borate buffer solution (see Supporting Information, Figure SP2). Figure 3a shows the temperature variations along the center line of the microchannel after applying 1200 V, and Figure 3b shows the temperature distribution at 5 min (inverse false color image of rhodamine B solution). As expected, the temperature near the narrowest region of the channel is higher than the wider regions. However, the highest temperature point is slightly off-center because of convectional heat transfer from the electroosmotic flow. At the beginning of the run, the temperature increase is quite fast but the rate slows with time. Establishing this temperature profile required only ~25 J of energy, which is ~1/80th of the energy needed to obtain the same profile using external thermoelectric heat sinks, thus supporting the low-power advantage of this system.

Temperature Gradient Focusing by Joule Heating. Several focusing experiments were performed with two model analytes (fluorescein−Na and FITC−BSA; both of them are negatively charged at the buffer pH values used) in 900 mM Tris−borate buffer in the microdevice. Parts a and b in Figure 4 show the focusing of fluorescein−Na and FITC−BSA after applying 1200 V for 5 min in individual runs, respectively. Initially, the microchannel was filled with a diluted sample solution uniformly distributed within the channel. After high electric potential was applied to the channel, the analytes were slowly focused at the central region of the microchannel and the analyte concentration increased at this location. Note that the symmetric geometry of the channel yields two locations where $u_{net} = 0$, but the focusing condition that $\partial u_{net}/\partial x < 0$ only occurs at one of these points. Species depletion results at the other location.

The preconcentration capability of this system was investigated by comparing the fluorescence intensity of the focused sample with that of several standard concentration samples (5, 10, and 20 μM). Figure 5 shows the concentration of 100 nM FITC−BSA due to an applied 1200 V in the microchannel. At least 200-fold concentration was achieved in just 2 min. Fluorescence intensity is measured at the location of maximum intensity over the entire microchannel because the focused sample plug is quite wide and the intensity is not uniform within this plug.

The same focusing experiments were performed with both model analytes diluted with 20 mM phosphate buffer, but stable focusing was not achieved. The temperature-dependent mobility curve in Figure 2b shows that focusing should be possible with this buffer as long as a sufficient temperature profile can be reached such that the concentration conditions are met. However, the conductivity of the phosphate buffer is ~3 times that of the 900 mM Tris−borate buffer at room temperature and increases 1.5 times faster with temperature (empirical results). The higher

conductivity creates "thermal runaway" control problems in achieving a stable temperature profile as the increased conductivity at higher temperatures induces more Joule heating and, of course, an even higher temperature. This condition led to rapid boiling in the microchannel and hindered all focusing attempts. When a lower voltage was applied to prevent boiling, an insufficient temperature profile resulted and focusing was not possible. Focusing experiments were also attempted in more dilute phosphate buffers (5 and 10 mM) to reduce the conductivity. Although the thermal runaway is alleviated, focusing was not achieved most likely because lower buffer concentration also reduces the ζ potential at the channel walls, thus lowering the bulk fluid velocity. Further experimentation is required to analyze the tradeoff between buffer conductivity and resulting ζ potential.

An interesting phenomenon occurring during the focusing process was that the focused sample plug slowly moved toward the anode side and finally disappeared from the viewing area. One possible explanation is that because a steady-state temperature profile is difficult to achieve, the temperature may be continually increasing in this region and the electrophoretic mobility of the sample analyte may be dominant over the bulk flow, as seen in Figure 2a. The location where the net velocity of the analyte reaches zero moves away from the horizontal center of the microchannel because the temperature of the sample solution keeps increasing due to the continuous electric current. In most focusing experiments using 1200 V applied with 900 mM Tris−borate buffer, we were able to maintain a focused plug for 15−20 min before the instability ensued.

The temperature gradient in our system is generated via Joule heating through varying channel geometry, and the temperature within the microchannel keeps increasing until the electric field is removed or the sample solution boils. To prevent the sample solution from boiling and migration of the focused sample plug, the current flowing through the microchannel was manually controlled by changing the applied electric potential. When the sample analyte started to focus, the voltage was lowered to keep the current magnitude stable and the focused sample plug remained idle. However, if the voltage is lowered too much, the temperature gradient is not sufficient to achieve zero net velocity and the focused sample plug moves toward the cathode side due to higher electroosmotic flow. The sample plug movement is very sensitive to the current intensity (i.e., the temperature variation); thus, proper current control is required for well-maintained sample focusing.

The focusing of a mixture of two analytes was performed to show the separation capability of the temperature gradient via Joule heating. Two analytes (25 μM fluorescein−Na and 100 nM FITC−BSA) were diluted in 900 mM Tris−borate buffer and concurrently focused at the same location for 5 min by 1200 V of electric potential (Figure 6a and b) and subsequently separated due to the mobility difference for $t > 5$ min (Figure 6a and c). Because of the difficulty in achieving a steady-state temperature profile, the temperature along the channel continually increases due to the constant electric field. As evident in Figure 2a, electrophoresis begins to dominate at higher temperatures and thus the species begin to drift toward the anode. During this separation process, the two focused plugs slowly migrate toward the anode side at different rates due to the dissimilar electrophoretic mobilities of the analytes, and the separation distance between the two plugs increased. The movement of the analytes lessens the concentration of the focused plugs, due to the increasing channel width and diffusion, but enhances the separation of the two species. The increasing distance between two plugs may also be caused by the widening channel, which reduces the electroosmotic flow opposing the electrophoretic movement of negatively charged molecules.

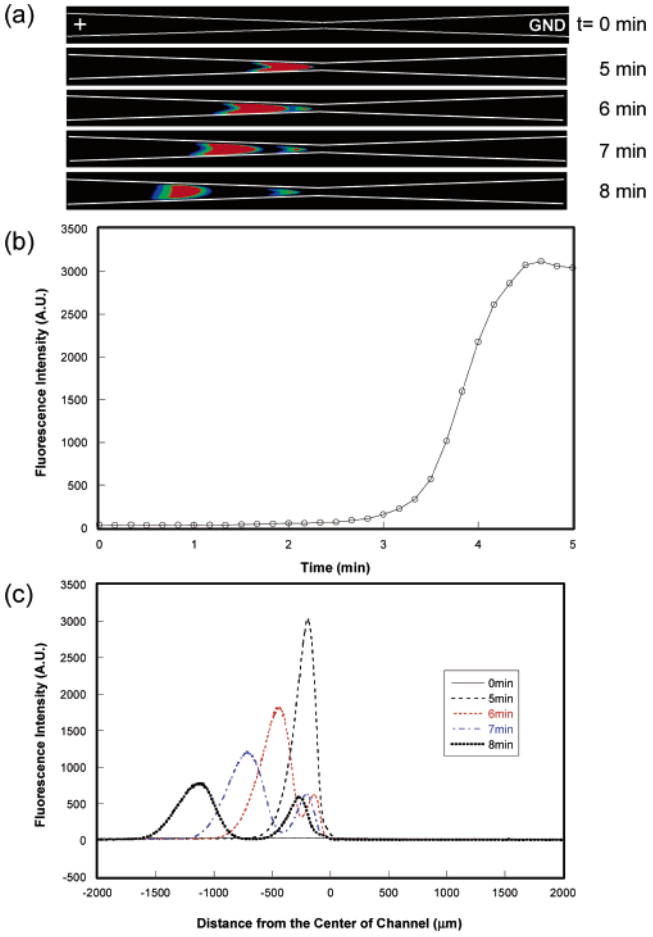

Figure 6. Time sequence images and fluorescence intensity profiles during separation of a mixture of 25 μM fluorescein−Na and 100 nM FITC-BSA in 900 mM Tris−borate buffer due to applied 1200 V electric potential. (a) Time sequence images show the separation of the two species over time. Both species were focused at the same area until $t = 5$ min and subsequently separated due to the mobility difference for $t > 5$ min. (b) Plot shows the maximum fluorescence intensity along centerline of microchannel during concurrent focusing of fluorescein and FITC−BSA. (c) Plot shows the fluorescence intensity variations along centerline of microchannel over time.

Perhaps a more powerful method of species separation using this device involves coupling species preconcentration with a subsequent electrophoretic separation along the same channel (see Supporting Information, Figure SP3). Note that more difficult protein−protein separations were not performed in this device due to the short length of the channel. However, this concentration technique should be able to be coupled to almost any length separation system.

Temperature Importance and TGF with More Common Buffers. The dominant factor governing the focusing and separation of analytes is the temperature gradient within the microchan-

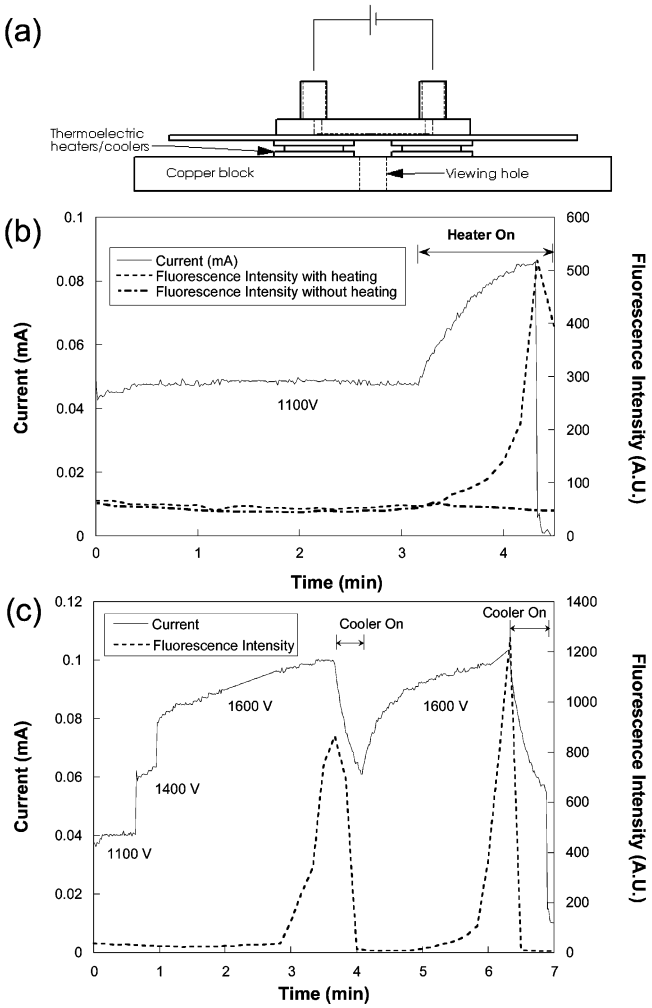

Figure 7. Focusing of 0.1 mM fluorescein−Na in 900 mM Tris−borate buffer using combination of Joule heating and external heating/cooling. (a) Schematic drawing showing the system composed of a copper block, two thermoelectric heat sinks, and the experimental microdevice from Figure 1. (b) Heating experiment: 1100 V electric potential was applied for 3 min. Sample focusing began after applying external heating for $t > 3$ min with constant 1100 V electric potential. Solid line, current; dashed line, florescence intensity with heating; and dash−dot line, fluorescence intensity without heating. (c) Cooling experiment: sample focusing was achieved by applying a 1600 V electric potential, but the focused sample plug disappeared when external cooling was applied. Solid line, current; and dashed line, fluorescence intensity.

nel caused by Joule heating due to the electric field. To validate the temperature effect on the focusing mechanism, an experimental setup incorporating thermoelectric heat sinks was developed as shown in Figure 7a.

At first, the heat sinks were used to heat the sample solution within the microchannel. Figure 7b shows the profile of the current and the fluorescence intensity of the 0.1 mM fluorescein−Na diluted in 900 mM Tris−borate buffer. Focusing of the sample was not achieved by simply applying an 1100 V electric potential for 3 min and the current remained quite stable, implying that there is little temperature increase. Sample focusing began after applying external heating (∼45 °C) for $t > 3$ min with constant 1100 V electric potential still applied to the microchannel. The solution in the microchannel began boiling when the temperature reached the boiling point (∼100 °C) and the focused plug abruptly disappeared. Sample focusing did not occur during the same time frame with only the 1100 V electric potential, as the dash−dot line shows in Figure 7b. The electric potential alone is not enough to form the temperature gradient in the microchannel needed to obtain sample focusing.

Next, a similar experiment was performed using the thermoelectric heat sinks to cool the microdevice. Sample focusing was achieved by applying a 1600 V electric potential, but the focused sample plug disappeared when external cooling (∼10 °C) was applied (in Figure 7c). The sample was focused again after the external cooling was turned off, and the focusing disappeared again due to external cooling.

Focusing experiments were attempted again with fluorescein−Na diluted in 20 mM phosphate buffer using the combined Joule heating and external heater system. The external heater was used to increase the base temperature up to 40 °C, and the applied potential to the microchannel was ramped up from 250 to 600 V over 10 min. A >10-fold focusing of sample analyte was achieved after 10 min (see Supporting Information, Figure SP4). In a combined Joule heating and external heater system, a steady-state temperature profile can be more readily achieved in a microchannel compared to a system only using Joule heating. The external heater elevates the base temperature of the microchannel, thus reducing the Joule heating, or electric potential, needed for focusing of analytes. Due to the low electric potential required for achieving the necessary temperature, the temperature profile can be more stable than a system without the external heater, and higher conductivity buffer solutions can be employed for TGF. The focused plug, however, drifted toward the left side of the channel slowly after focusing in the middle. We need further study to resolve this drifting problem in phosphate buffer system, as the cause of this drift is still unclear.

CONCLUSION AND FUTURE WORK

In this work, we have presented an analysis of temperature-dependent transport behavior along a microchannel and used the theory to develop a simple TGF device exploiting an inherent Joule heating effect. Our variable-width PDMS device delivers rapid and repeatable focusing of model analytes using relatively low power compared to current TGF approaches. However, maintaining a steady-state temperature profile with this system was difficult due to the thermal runaway induced by the increasing buffer conductivity with temperature. This effect led to difficulty in achieving a stable and maintained concentration, elucidating the need for a more controlled system. We are currently designing a feedback system to control the current through the system and negate any thermal runaway.

Our combined Joule heating with external heating/cooling experiments strongly suggests that temperature indeed is the dominant factor in achieving focusing. Future work will involve employing that technique to focus molecules in systems otherwise thought impossible. For instance, we showed that the 900 mM Tris−borate buffer is more conducive to TGF than the 20 mM phosphate buffer because it is less conductive yet yields steeper $\partial\mu_{net}/\partial T$ curves. However, the combined system device may allow for better focusing using the 20 mM phosphate buffer as it can more precisely control temperature and prevent thermal runaway commonly seen.

The device was used to concentrate and separate two species in solution, 25 μM fluorescein−Na and 100 nM FITC−BSA, in less than 10 min. Future research will include using the technique to achieve more interesting separations, such as an on-line immunoassay. We recognize that the high temperatures currently used to achieve focusing will most likely be harmful to more sensitive biomolecules, but we are optimistic that a future design will yield nondestructive separations using this simple, repeatable technique.

ACKNOWLEDGMENT

The authors acknowledge the National Institute of Dental and Craniofacial Research under NIH (Grant 1 U01 DE14961-01) for funding S.M.K., as well as the U.S. Department of Homeland Security Fellowship Program for funding G.J.S. We also thank Meng Ping Chang for help in designing the photobleached dye imaging method, and Roel Huerta for developing the mobility calculation Matlab code. S.M.K. and G.J.S. contributed equally to the manuscript.

SUPPORTING INFORMATION AVAILABLE

Additional information as noted in text. This material is available free of charge via the Internet at http://pubs.acs.org.

Received for review July 1, 2006. Accepted September 15, 2006.

AC061194P